

Characterizing Non-Gaussian Features of Acid Concentrations in a Spent Fuel Dissolver Model

James J. Peltz¹ and Dan G. Cacuci²

¹Karlsruhe Institute of Technology, IFRT, Vincent-Priessnitz-Str., 76131 Karlsruhe, Germany

²University of South Carolina, Center for Nuclear Science and Energy, 541 Main Street, Columbia, SC, 29208, USA

Abstract - This paper quantifies second-order response sensitivities for a deterministic spent nuclear fuel dissolver model, a model representing a likely mechanical component of an aqueous nuclear fuel separation facility. Results show large negatively skewed response distributions for several dissolver parameters, i.e., smaller than expected values of for computed nitric acid concentrations and discusses these results in the context of Gaussian-based confidence intervals used to support decision making. This paper compliments several previous numerical studies¹⁻⁴ using the general forward and inverse predictive modeling methodology of Cacuci and Ionescu-Bujor⁵.

I. INTRODUCTION

The basic motivation for pursuing research and development in support of nuclear nonproliferation and international nuclear safeguards is to make informed decisions on a target of interest where the ability to collect accurate data are limited due to potential physical and political constraints. When considering using measured or computed data to inform such efforts, it should be understood that extracting “best estimate” values for model parameters and predicted results (responses), together with “best estimate” uncertainties requires reasoning from incomplete, error-afflicted, and occasionally discrepant information⁵. Quantifying uncertainties that accompanying these measurements and computations are essential to understanding how well the available information answers specific questions regarding the domain of interest, and the risk posed by using such information by what is unknown.

Central to the results presented here is Cacuci’s adjoint sensitivity analysis methodology (ASAM)⁵⁻⁸ which computes exact model response sensitivities for model parameters. These “sensitivities” support a wide range of efforts related to model validation such as: (1) understanding the system by identifying and ranking the importance of model parameters in influencing the response under consideration; (2) determining the effects of parameter variations on the system’s behavior thus improving the system design, possibly reducing conservatism and redundancy; (3) prioritizing possible improvements for the system under consideration by quantifying uncertainties in responses due to quantified parameter uncertainties; and (4) performing “predictive modeling”, including data assimilation and model calibration, for the purpose of obtaining best-estimate predicted results with reduced predicted uncertainties⁸.

The spent nuclear fuel dissolver model comprises 16 coupled nonlinear first-order equations that describe the time-evolution of the volumetric mass concentration of nitric acid of the liquid phase. The number of imprecisely

known scalar model parameters is 1291, for which only the nominal values and the corresponding standard deviations are known. Previous numerical studies document the validation and uncertainty quantification of the dissolver model are published and available for better context of using the general forward and inverse predictive modeling methodology¹⁻⁴ and its utility to potentially provide a full description of errors from both models and measurements⁵.

This paper is organized as follows: Section 2 provides a brief discussion regarding the dissolver model’s base case at compartment #1 using spectral representations of an operator type response for computing most efficiently exact 1st order sensitivities developed by Cacuci⁹; Section 3 articulates the methodology for quantifying mixed 2nd order response sensitivities which are essential for characterizing the skewness of the model response distribution and thus a description of non-Gaussian features for computed nitric acid concentrations; Section 4, shows and discusses results for these 2nd order sensitivities and their effect on the “skewness” of the response distribution; and Section 5 concludes with a brief discussion on the importance of having these higher order moments when using models and measurements for decision making.

II. DISSOLVER MODEL 1ST ORDER SENSITIVITIES

The dissolver model comprises 1291 model parameters: $\rho_a^{(in)}(t_0), \dots, \rho_a^{(in)}(t_{635}), \dot{m}^{(in)}(t_0), \dots, \dot{m}^{(in)}(t_{635})$, represented in Figure 1, and 16 initial conditions $\rho_a^{(k)}(0)$ and $V^{(k)}(0)$, as well as the parameters a, b, V_0, p, G .

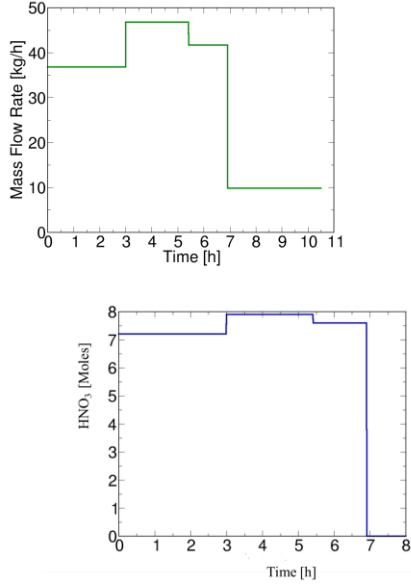


Fig. 1. **Top:** Dissolver Model parameters Inlet Mass Flow Rate $\rho_a^{(in)}(t_0)$ **Bottom:** Inlet Nitric Acid Concentration $\dot{m}^{(in)}(t_0)$.

Particularly important scalar-valued responses for the dissolver model are the measured and/or computed nitric acid concentration in a compartment k at a time-instance t_i :

$$\rho_a^{(k)}(t_i) = \int_0^{t_f} \rho_a^{(k)}(t) \delta(t-t_i) dt \quad (1)$$

The sensitivity of the nitric acid concentration in compartment #1 can be obtained by computing the (first-order) Gateaux-differential⁵⁻⁷ of Eq. (1), given by the following expression:

$$\delta \rho_a^{(k)}(t_i) = \int_0^{t_f} \Delta \rho_a^{(k)}(t) \delta(t-t_i) dt, \quad i = 1, \dots, I \quad (2)$$

where $\Delta \rho_a^{(k)}(t)$ represents an arbitrary variation in the respective concentration. Previous numerical studies on the dissolver demonstrate ASAM for a nonlinear system⁶ and “ASAM for operator-type responses”¹⁰ respectively. The “ASAM for operator-type responses” considers the spectral representation of an operator-type (e.g., time and/or pace dependent) response. The response $\rho_a^{(k)}(t)$ defined in Eq. (1) admits the following N^{th} -order spectral expansion $\rho_{a,s}^{(k)}(t)$ (where the subscript “S” indicates “spectral”):

$$\rho_{a,s}^{(k)}(t) = \sum_{n=0}^N a_n P_n(2t/t_f - 1), \quad 0 < t \leq t_f, \quad (3)$$

with

$$a_n = \frac{2n+1}{t_f} \int_0^{t_f} \rho_{a,s}^{(k)}(t) P_n(2t/t_f - 1) dt, \quad n = 0, 1, \dots, N. \quad (4)$$

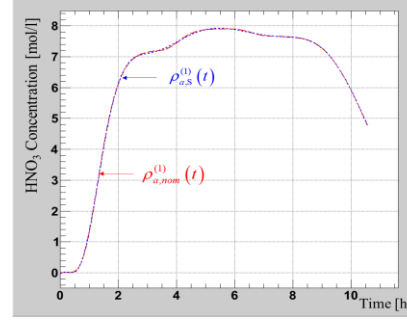


Fig. 2. Time-dependent behavior of the exact nitric acid concentration in compartment #1, $\rho_{a,s}^{(1)}(t)$, and its spectral representation, $\rho_{a,s}^{(1)}(t)$, using the first 17 Legendre polynomials.

Figure 2 (above) shows computed model responses using the first 17 Legendre polynomials and the full 1291 parameters. The spectral representation $\rho_{a,s}^{(1)}(t)$ of $\rho_a^{(1)}(t)$ is shown to differ by less than 1% over the duration of the transient (10.5 hours, or 635 computational steps of 1 minute).

Previous numerical studies⁷ developed the 1st order adjoint sensitivity system and its solution vector i.e., the adjoint function as $\Psi(t) \square [\Psi_\rho(t), \Psi_V(t)]$:

$$\begin{aligned} \delta R(\mathbf{u}^0, \boldsymbol{\alpha}^0; \boldsymbol{\psi}, \mathbf{h}_\alpha) = & \sum_{k=1}^8 \int_0^{t_f} \psi_\rho^{(k)}(t) q_\rho^{(k)}(t) dt \\ & + \sum_{k=1}^8 \int_0^{t_f} \psi_V^{(k)}(t) q_V^{(k)}(t) dt \\ & + \sum_{k=1}^8 \left\{ \psi_\rho^{(k)}(0) V_{nom}^{(k)}(0) [\Delta \rho_{a0}^{(k)}] + \psi_V^{(k)}(0) [\Delta V_0^{(k)}] \right\}. \end{aligned} \quad (5)$$

As equation 5 indicates, the sensitivities $\delta R(\mathbf{u}^0, \boldsymbol{\alpha}^0; \boldsymbol{\psi}, \mathbf{h}_\alpha)$ to all system parameters can be computed after the adjoint sensitivity system is solved once and corresponding adjoint functions, $\Psi \square [\Psi_\rho, \Psi_V]$, are obtained. Moreover, for computing sensitivities with operator type responses for the nitric acid concentration, $\delta \rho_{a,s}^{(1)}(t)$, takes on the form:

$$\delta\rho_{a,s}^{(1)}(t) = \sum_{n=0}^{N=16} \delta a_n(\mathbf{h}_\alpha, \boldsymbol{\psi}; \boldsymbol{\alpha}^0) P_n(2t/t_f - 1), \quad (6)$$

where

$$\begin{aligned} \delta a_n(\mathbf{h}_\alpha, \boldsymbol{\psi}; \boldsymbol{\alpha}^0) = & \sum_{k=1}^8 \int_0^{t_f} \psi_{\rho,n}^{(k)}(t) q_{\rho}^{(k)}(t) dt + \sum_{k=1}^8 \int_0^{t_f} \psi_{V,n}^{(k)}(t) q_V^{(k)}(t) dt \\ & + \sum_{k=1}^8 \left\{ \psi_{\rho,n}^{(k)}(0) V_{nom}^{(k)}(0) [\Delta\rho_{a0}^{(k)}] + \psi_{V,n}^{(k)}(0) [\Delta V_0^{(k)}] \right\}, \\ & n = 0, 1, \dots, N = 16. \end{aligned} \quad (7)$$

Equations 6 and 7 are used to compute sensitivities of the nitric acid concentration in compartment #1 but can also be used to compute the relative sensitivities for the other compartments. Only the relative sensitivities for $\dot{m}^{(in)}(t_i)$ and $\rho_a^{(in)}(t_i)$ are shown in this work. Figure 3 shows the relative sensitivities for, $\dot{m}^{(in)}(t_i)$ and $\rho_a^{(in)}(t_i)$, at specific time instances for compartment #1.

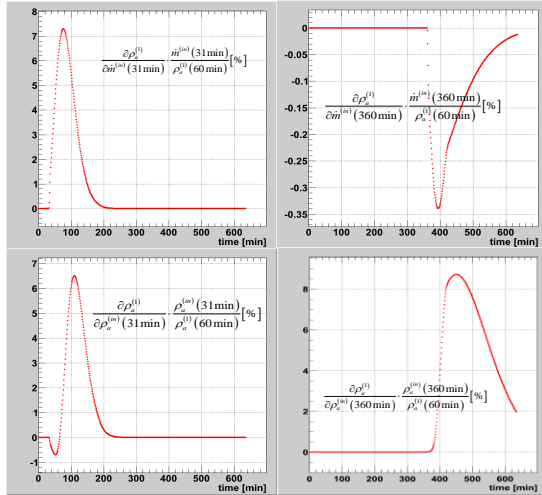


Fig. 3. Relative sensitivities of $\rho_{a,nom}^{(1)}(t_i)$ for the scalar parameters $\dot{m}^{(in)}(t_i)$ and $\rho_a^{(in)}(t_i)$, at times 31 and 360 mins in compartment #1.

The relative sensitivities were calculated for all scalar parameters at several time steps over the full transient for compartments #1, #4, and #7 as published in the predictive modeling study¹. These sensitivities were also used to understand numerous trends which were used to inform the 2nd order sensitivity analyses to be discussed in the subsequent sections of this paper.

III. SKEWNESS AND NON-GAUSSIAN FEATURES OF THE NITRIC ACID CONCENTRATIONS

Recall the spent nuclear fuel dissolver model comprises 16 coupled nonlinear first-order equations that describe the time-evolution of the volumetric mass concentration of nitric acid of the liquid phase, as shown in Figures 1 and 2. The number of imprecisely known scalar model parameters is 1291, for which only the nominal values and the corresponding standard deviations are known. Recall, all parameters are considered to be all uncorrelated and normally distributed as shown previously in Section 2.

Assuming an uncorrelated and normally distributed parameter distribution function, the mean, covariance, variance, and higher order moments as can be simplified as.

$$[E(r_k)]^{UG} = r_k(\boldsymbol{\alpha}^0) + \frac{1}{2} \sum_{i=1}^{N_\alpha} \frac{\partial^2 r_k}{\partial \alpha_i^2} \sigma_i^2 \quad (8)$$

$$\begin{aligned} [cov(r_k, r_l)]^{UG} = & \sum_{i=1}^{N_\alpha} \left(\frac{\partial r_k}{\partial \alpha_i} \frac{\partial r_l}{\partial \alpha_i} \right) \sigma_i^2 \\ & + \frac{1}{2} \sum_{i=1}^{N_\alpha} \left(\frac{\partial^2 r_k}{\partial \alpha_i^2} \right) \left(\frac{\partial^2 r_l}{\partial \alpha_i^2} \right) \sigma_i^4. \end{aligned} \quad (9)$$

$$[\text{var}(r_k)]^{UG} = \sum_{i=1}^{N_\alpha} \left(\frac{\partial r_k}{\partial \alpha_i} \right)^2 \sigma_i^2 + \frac{1}{2} \sum_{i=1}^{N_\alpha} \left(\frac{\partial^2 r_k}{\partial \alpha_i^2} \right)^2 \sigma_i^4. \quad (10)$$

$$[\mu_3(r_k)]^{UG} = 3 \sum_{i=1}^{N_\alpha} \left(\frac{\partial r_k}{\partial \alpha_i} \right)^2 \frac{\partial^2 r_k}{\partial \alpha_i^2} \sigma_i^4. \quad (11)$$

where the superscript ‘‘UG’’ indicates ‘‘uncorrelated Gaussian’’ parameters. Expressions 8-11 indicate the 2nd order sensitivities have the following impacts on the response moments: (1) they cause the ‘‘expected value of the response, $[E(r_k)]^{UG}$, to differ from the computed nominal value of the response’’, $r_k(\boldsymbol{\alpha}^0)$; (2) they contribute to the response variances and covariances; however, since the contributions involving the second-order sensitivities are multiplied by the fourth power of the parameters’ standard deviations, the total of these contributions is expected to be relatively smaller compared to the contributions of the first-order response sensitivities; and (3) the 2nd-order sensitivities provide the leading contributions to the third-order moment, $[\mu_3(r_k)]^{UG}$, and –hence the skewness, a response that depends on *uncorrelated and normally distributed* parameters.

The above relations are also valid when the parameters and/or responses are implicit functions of time, as is the case for the acid concentration responses $\rho_a^{(k)}(t_i)$, $k=1, \dots, 8$, which are functions of 1291 scalar parameters. If the inlet mass rate flow $\dot{m}^{(in)}(t_i)$ and the inlet

acid concentration $\rho_a^{(in)}(t_i)$ are considered to vary independently at every time node t_i , $i = 1, \dots, 635$ then:

$$\frac{\partial \rho_a^{(k)}(t_i; \mathbf{a}^0)}{\partial \rho_a^{(in)}(t_j)} = 0, \quad \frac{\partial \rho_a^{(k)}(t_i; \mathbf{a}^0)}{\partial \dot{m}^{(in)}(t_j)} = 0, \quad j > i, \quad i = 1, \dots, 635;$$

$$\frac{\partial^2 \rho_a^{(k)}(t_i; \mathbf{a}^0)}{\partial [\rho_a^{(in)}(t_j)]^2} = 0, \quad \frac{\partial^2 \rho_a^{(k)}(t_i; \mathbf{a}^0)}{\partial [\dot{m}^{(in)}(t_j)]^2} = 0, \quad j > i, \quad i = 1, \dots, 635.$$

(12)

and

$$\dot{m}^{(in)}(t) = \begin{cases} \dot{m}_A, & t_0 \leq t < t_A \\ \dot{m}_B, & t_A \leq t < t_B \\ \dot{m}_C, & t_C \leq t < t_D \\ \dot{m}_D, & t_D \leq t < t_f \end{cases}; \quad \rho_a^{(in)}(t) = \begin{cases} \rho_{a,A}^{(in)}, & t_0 \leq t < t_A \\ \rho_{a,B}^{(in)}, & t_A \leq t < t_B \\ \rho_{a,C}^{(in)}, & t_C \leq t < t_D \\ \rho_{a,D}^{(in)}, & t_D \leq t < t_f \end{cases}$$

(13)

Which means that the time dependent acid concentrations do depend on parameters from future time steps and that $\dot{m}^{(in)}(t)$ and $\rho_a^{(in)}(t)$ do not vary independently at each time step, but are piecewise constant functions as verified by Figure 1. Consequently, equations. 8, 10, and 11 take on the following form for the expectation for the time-dependent acid concentration, $\rho_a^{(k)}(t_i)$, $k = 1, \dots, 8$, in each of the eight compartments:

The expectation, $E[\rho_a^{(k)}(t_i; \mathbf{a}^0)]$, of $\rho_a^{(k)}(t_i; \mathbf{a}^0)$:

$$E[\rho_a^{(k)}(t_i; \mathbf{a}^0)] = \rho_a^{(k)}(t_i; \mathbf{a}^0) + E_2[\rho_a^{(k)}(t_i; \mathbf{a}^0)], \quad (14)$$

$k = 1, \dots, 8; \quad i = 1, \dots, 635;$

where the quantity $E_2[\rho_a^{(k)}(t_i; \mathbf{a}^0)]$ comprises the 2nd-order contributions to the expectation $E[\rho_a^{(k)}(t_i; \mathbf{a}^0)]$ and is defined as:

$$E_2[\rho_a^{(k)}(t_i; \mathbf{a}^0)] \square \frac{1}{2} \frac{\partial^2 \rho_a^{(k)}(t_i; \mathbf{a}^0)}{\partial a^2} \text{var}(a) + \frac{1}{2} \frac{\partial^2 \rho_a^{(k)}(t_i; \mathbf{a}^0)}{\partial b^2} \text{var}(b) + \frac{1}{2} \frac{\partial^2 \rho_a^{(k)}(t_i; \mathbf{a}^0)}{\partial V_0^2} \text{var}(V_0) + \frac{1}{2} \frac{\partial^2 \rho_a^{(k)}(t_i; \mathbf{a}^0)}{\partial p^2} \text{var}(p) + \frac{1}{2} \frac{\partial^2 \rho_a^{(k)}(t_i; \mathbf{a}^0)}{\partial G^2} \text{var}(G) + X(k; t_i) + \frac{1}{2} \sum_{j=1}^8 \left\{ \frac{\partial^2 \rho_a^{(k)}(t_i; \mathbf{a}^0)}{\partial [\rho_a^{(j)}(0)]^2} \text{var}[\rho_a^{(j)}(0)] + \frac{\partial^2 \rho_a^{(k)}(t_i; \mathbf{a}^0)}{\partial [V^{(j)}(0)]^2} \text{var}[V^{(j)}(0)] \right\},$$

for $k = 1, \dots, 8; \quad i = 1, \dots, 635;$

(15)

where the quantity $X(k; t_i)$ is defined for

$k = 1, \dots, 8; \quad i = 1, \dots, 635$, as follows:

$$X(k; t_i) \square \frac{1}{2} \left\{ \frac{\partial^2 \rho_a^{(k)}(t_i; \mathbf{a}^0)}{\partial [\rho_{a,A}^{(in)}]^2} \text{var}[\rho_{a,A}^{(in)}] + \frac{\partial^2 \rho_a^{(k)}(t_i; \mathbf{a}^0)}{\partial [\dot{m}_A]^2} \text{var}[\dot{m}_A] \right\}, \quad \text{for } t_0 \leq t_i < t_A;$$

(16)

$$X(k; t_i) \square \frac{1}{2} \left\{ \frac{\partial^2 \rho_a^{(k)}(t_i; \mathbf{a}^0)}{\partial [\rho_{a,A}^{(in)}]^2} \text{var}[\rho_{a,A}^{(in)}] + \frac{\partial^2 \rho_a^{(k)}(t_i; \mathbf{a}^0)}{\partial [\dot{m}_A]^2} \text{var}[\dot{m}_A] \right\} + \frac{1}{2} \left\{ \frac{\partial^2 \rho_a^{(k)}(t_i; \mathbf{a}^0)}{\partial [\rho_{a,B}^{(in)}]^2} \text{var}[\rho_{a,B}^{(in)}] + \frac{\partial^2 \rho_a^{(k)}(t_i; \mathbf{a}^0)}{\partial [\dot{m}_B]^2} \text{var}[\dot{m}_B] \right\}, \quad \text{for } t_A \leq t_i < t_B;$$

(17)

$$\begin{aligned}
 X(k; t_i) \square & \frac{1}{2} \left\{ \frac{\partial^2 \rho_a^{(k)}(t_i; \mathbf{\alpha}^0)}{\partial [\rho_{a,A}^{(in)}]^2} \text{var}[\rho_{a,A}^{(in)}] \right. \\
 & \left. + \frac{\partial^2 \rho_a^{(k)}(t_i; \mathbf{\alpha}^0)}{\partial [\dot{m}_A]^2} \text{var}[\dot{m}_A] \right\} \\
 & + \frac{1}{2} \left\{ \frac{\partial^2 \rho_a^{(k)}(t_i; \mathbf{\alpha}^0)}{\partial [\rho_{a,B}^{(in)}]^2} \text{var}[\rho_{a,B}^{(in)}] \right. \\
 & \left. + \frac{\partial^2 \rho_a^{(k)}(t_i; \mathbf{\alpha}^0)}{\partial [\dot{m}_B]^2} \text{var}[\dot{m}_B] \right\} \\
 & + \frac{1}{2} \left\{ \frac{\partial^2 \rho_a^{(k)}(t_i; \mathbf{\alpha}^0)}{\partial [\rho_{a,C}^{(in)}]^2} \text{var}[\rho_{a,C}^{(in)}] \right. \\
 & \left. + \frac{\partial^2 \rho_a^{(k)}(t_i; \mathbf{\alpha}^0)}{\partial [\dot{m}_C]^2} \text{var}[\dot{m}_C] \right\}, \text{ for } t_B \leq t_i < t_C;
 \end{aligned} \tag{18}$$

$$\begin{aligned}
 X(k; t_i) \square & \frac{1}{2} \left\{ \frac{\partial^2 \rho_a^{(k)}(t_i; \mathbf{\alpha}^0)}{\partial [\rho_{a,A}^{(in)}]^2} \text{var}[\rho_{a,A}^{(in)}] \right. \\
 & \left. + \frac{\partial^2 \rho_a^{(k)}(t_i; \mathbf{\alpha}^0)}{\partial [\dot{m}_A]^2} \text{var}[\dot{m}_A] \right\} \\
 & + \frac{1}{2} \left\{ \frac{\partial^2 \rho_a^{(k)}(t_i; \mathbf{\alpha}^0)}{\partial [\rho_{a,B}^{(in)}]^2} \text{var}[\rho_{a,B}^{(in)}] \right. \\
 & \left. + \frac{\partial^2 \rho_a^{(k)}(t_i; \mathbf{\alpha}^0)}{\partial [\dot{m}_B]^2} \text{var}[\dot{m}_B] \right\} \\
 & + \frac{1}{2} \left\{ \frac{\partial^2 \rho_a^{(k)}(t_i; \mathbf{\alpha}^0)}{\partial [\rho_{a,C}^{(in)}]^2} \text{var}[\rho_{a,C}^{(in)}] \right. \\
 & \left. + \frac{\partial^2 \rho_a^{(k)}(t_i; \mathbf{\alpha}^0)}{\partial [\dot{m}_C]^2} \text{var}[\dot{m}_C] \right\} \\
 & + \frac{1}{2} \left\{ \frac{\partial^2 \rho_a^{(k)}(t_i; \mathbf{\alpha}^0)}{\partial [\rho_{a,D}^{(in)}]^2} \text{var}[\rho_{a,D}^{(in)}] \right. \\
 & \left. + \frac{\partial^2 \rho_a^{(k)}(t_i; \mathbf{\alpha}^0)}{\partial [\dot{m}_D]^2} \text{var}[\dot{m}_D] \right\}, \text{ for } t_C \leq t_i < t_D.
 \end{aligned} \tag{19}$$

The variance, $\text{Var}[\rho_a^{(k)}(t_i; \mathbf{\alpha}^0)]$, of $\rho_a^{(k)}(t_i; \mathbf{\alpha}^0)$:

$$\begin{aligned}
 \text{Var}[\rho_a^{(k)}(t_i; \mathbf{\alpha}^0)] & = \text{Var}_1[\rho_a^{(k)}(t_i; \mathbf{\alpha}^0)] + \text{Var}_2[\rho_a^{(k)}(t_i; \mathbf{\alpha}^0)], \\
 k & = 1, \dots, 8; \quad i = 1, \dots, 635;
 \end{aligned} \tag{20}$$

where the quantities $\text{Var}_1[\rho_a^{(k)}(t_i; \mathbf{\alpha}^0)]$ and $\text{Var}_2[\rho_a^{(k)}(t_i; \mathbf{\alpha}^0)]$ comprise the 1st-order and, respectively, the 2nd-order contributions to the variance $\text{Var}[\rho_a^{(k)}(t_i; \mathbf{\alpha}^0)]$, and the 3rd-order moment, $\mu_3[\rho_a^{(k)}(t_i; \mathbf{\alpha}^0)]$, of $\rho_a^{(k)}(t_i; \mathbf{\alpha}^0)$ but also having the quantities $Y(k; t_i)$, and $Z(k; t_i)$ respectively for $\text{for } k = 1, \dots, 8; \quad i = 1, \dots, 635$, again which are similar in time and form of $X(k; t_i)$ as shown in expressions 16-19. The skewness, $\gamma_1[\rho_a^{(k)}(t_i; \mathbf{\alpha}^0)]$, of $\rho_a^{(k)}(t_i; \mathbf{\alpha}^0)$ takes the form:

$$\begin{aligned}
 \gamma_1[\rho_a^{(k)}(t_i; \mathbf{\alpha}^0)] \square & \mu_3[\rho_a^{(k)}(t_i; \mathbf{\alpha}^0)] / \left\{ \text{Var}[\rho_a^{(k)}(t_i; \mathbf{\alpha}^0)] \right\}^{3/2}, \\
 k & = 1, \dots, 8; \quad i = 1, \dots, 635.
 \end{aligned} \tag{21}$$

Only a few non mixed 2nd order response sensitivities are needed to compute the respective terms from the expressions, and since the quantities for $\text{Var}_1[\rho_a^{(1)}(t_i; \mathbf{\alpha}^0)]$ and $\text{Var}_1[\rho_a^{(7)}(t_i; \mathbf{\alpha}^0)]$ which were computed exactly using the ASAM in previously studies¹ so it's more expedient to compute the respective non-mixed 2nd-order response sensitivities by using forward computations in conjunction with finite difference formulas, at every time step t_i , $i = 1, \dots, 635$ as:

$$\begin{aligned}
 \frac{\partial^2 \rho_a^{(k)}(t_i; \mathbf{\alpha}^0)}{\partial [\rho_a^{(in)}(t_i)]^2} & \cong \frac{1}{[\Delta \rho_a^{(in)}(t_i)]^2} \left\{ \rho_a^{(k)}[t_i; \rho_a^{(in)}(t_i) + \Delta \rho_a^{(in)}(t_i)] \right. \\
 & \left. - 2\rho_a^{(k)}[t_i; \rho_a^{(in)}(t_i)] + \rho_a^{(k)}[t_i; \rho_a^{(in)}(t_i) - \Delta \rho_a^{(in)}(t_i)] \right\}, \\
 k & = 1, \dots, 8.
 \end{aligned} \tag{22}$$

IV. RESULTS

The relative and absolute 2nd-order sensitivities of the time-dependent acid concentrations $\rho_a^{(1)}(t_i; \mathbf{\alpha}^0)$ in compartment #1 (furthest from the inlet) and, respectively, $\rho_a^{(7)}(t_i; \mathbf{\alpha}^0)$ in compartment #7 (closest to the inlet) were computed for all parameters but are depicted for \dot{m}_A , the largest, as shown in Figure 4 below.

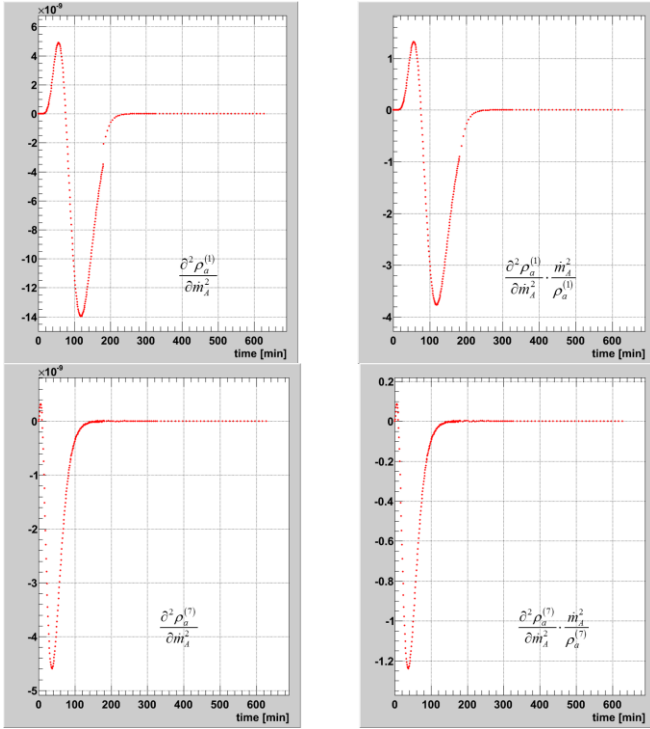


Fig. 4. Figure 4. Absolute (left) and relative (right) 2nd-order sensitivities of $\rho_a^{(1)}(t_i; \mathbf{\alpha}^0)$ (top) and $\rho_a^{(7)}(t_i; \mathbf{\alpha}^0)$ (bottom) with respect to \dot{m}_A , for $t_i, i = 1, \dots, 635$.

Some general trends for all of the computations performed indicate that: (1) the relative 2nd-order sensitivities are much smaller than the corresponding 1st-order sensitivities; (2) the largest are the relative 2nd-order sensitivity of $\rho_a^{(1)}(t_i; \mathbf{\alpha}^0)$ with respect to the model parameters $\dot{m}_A^{(in)}$, V_0 and b , at early times into the full transient, as well as to the model parameter $\dot{m}_D^{(in)}$, towards the end of the transient; (3) the 2nd-order sensitivities of the acid concentration in compartment #1 (furthest from the inlet) overall are larger than the corresponding 2nd-order sensitivities of the acid concentration in compartment #7 (closest to the inlet).

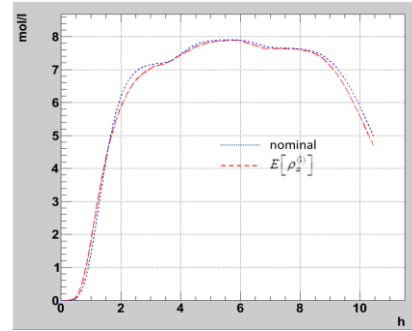


Fig. 5. Comparison of the nominal values $\rho_a^{(1)}(t_i; \mathbf{\alpha}^0)$ and $E[\rho_a^{(1)}(t_i; \mathbf{\alpha}^0)]$ for $t_i, i = 1, \dots, 635$.

Figure 5 illustrates the effects of the 2nd order sensitivities on the expectation values, $E[\rho_a^{(1)}(t_i; \mathbf{\alpha}^0)]$, of the acid concentration responses in the dissolvers compartments was found to be quite small. Figure 6 illustrates depicts the contributions of the 2nd-order sensitivities, contained in the quantity, $\text{var}_2[\rho_a^{(1)}(t_i; \mathbf{\alpha}^0)]$, to the variance of the acid concentration, $\rho_a^{(1)}(t_i; \mathbf{\alpha}^0)$, in compartment #1. This figure also depicts the minute influence of the 2nd-order sensitivities on the standard deviation of the acid concentration, $\rho_a^{(1)}(t_i; \mathbf{\alpha}^0)$, in compartment #1.

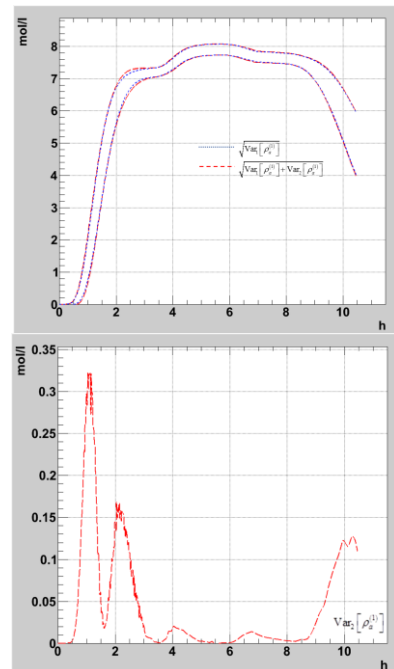


Fig.6. **Top:** Comparison of the standard deviation of $\rho_a^{(1)}(t_i; \mathbf{\alpha}^0)$ computed with 1st-order sensitivities vs. both 1st- and 2nd-order sensitivities, for $t_i, i = 1, \dots, 635$. **Bottom:**

Time-dependent variation of $\text{Var}_2[\rho_a^{(1)}(t_i; \mathbf{\alpha}^0)]$, cf. Eq. (20), for $t_i, i = 1, \dots, 635$.

The largest effects overall are on the expected value of the acid concentration in compartment #1. The individual contributions of the 2nd-order sensitivities to the most important model parameters and the *skewness* of the acid concentration responses $\rho_a^{(1)}(t_i; \mathbf{\alpha}^0)$ and $\rho_a^{(7)}(t_i; \mathbf{\alpha}^0)$ in compartments #1 and #7, furthest and closest to the inlet, respectively are depicted Figures 7-9. Figure 7 shows the negative distribution of $\rho_a^{(1)}(t_i; \mathbf{\alpha}^0)$ which occurs at ca. 3 hours into the transient which stems from the uncertainties in the (assumed) normally-distributed model parameter $\rho_{a,A}^{(in)}$. This behavior of notably large negative values for skewness in the distributions that occur in the middle of the transient for $\rho_a^{(1)}(t_i; \mathbf{\alpha}^0)$ and $\rho_a^{(7)}(t_i; \mathbf{\alpha}^0)$, induced by the parameters $\rho_{a,B}^{(in)}$ and $\rho_{a,C}^{(in)}$, respectively as shown by Figures 8 and 9.

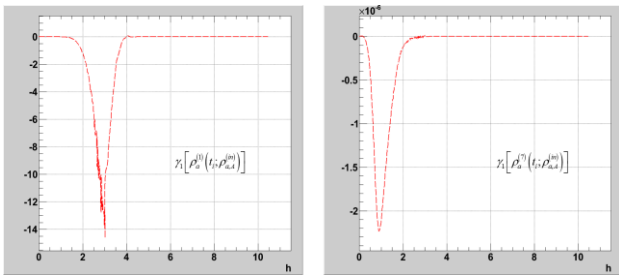


Fig. 7. Skewness in the distribution of $\rho_a^{(1)}(t_i; \mathbf{\alpha}^0)$ (left) and, respectively, $\rho_a^{(7)}(t_i; \mathbf{\alpha}^0)$ (right) due the uncertainties in the (assumed) normally-distributed model parameter $\rho_{a,A}^{(in)}$.

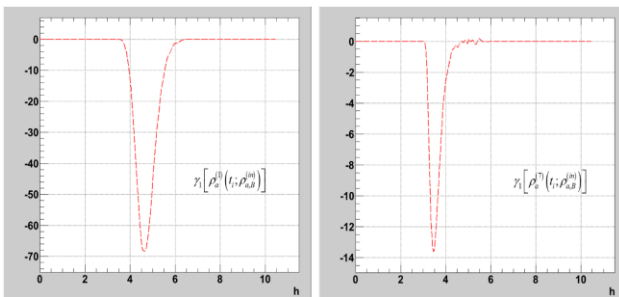


Fig. 8. Skewness in the distribution of $\rho_a^{(1)}(t_i; \mathbf{\alpha}^0)$ (left) and, respectively, $\rho_a^{(7)}(t_i; \mathbf{\alpha}^0)$ (right) due the uncertainties in the (assumed) normally-distributed model parameter $\rho_{a,B}^{(in)}$.

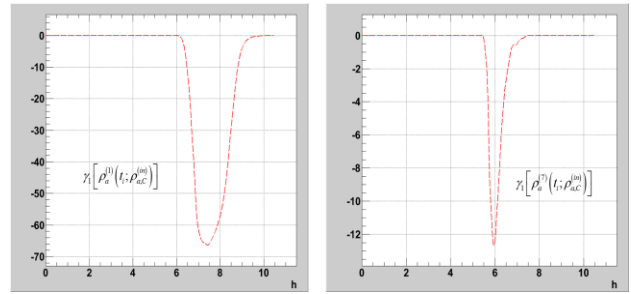


Fig. 9. Skewness in the distribution of $\rho_a^{(1)}(t_i; \mathbf{\alpha}^0)$ (left) and, respectively, $\rho_a^{(7)}(t_i; \mathbf{\alpha}^0)$ (right) due the uncertainties in the (assumed) normally-distributed model parameter $\rho_{a,C}^{(in)}$.

These highly negative values imply that the distributions of the responses $\rho_a^{(1)}(t_i; \mathbf{\alpha}^0)$ and $\rho_a^{(7)}(t_i; \mathbf{\alpha}^0)$ become heavily skewed toward smaller values than what would be calculated for the expected values. This behavior continues and increases by a factor of about 5 for the distribution of $\rho_a^{(1)}(t_i; \mathbf{\alpha}^0)$ in the compartment furthest from the inlet which again would imply smaller values than expected values. The cumulative impact of the uncertainties in the parameter distributions (assumed to be normal) on the skewness in the distributions of $\rho_a^{(1)}(t_i; \mathbf{\alpha}^0)$ and $\rho_a^{(7)}(t_i; \mathbf{\alpha}^0)$, respectively, are depicted in Figure 10.

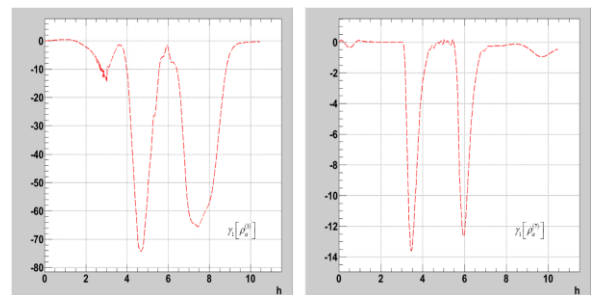


Fig. 10. Time-dependence of the total skewness, $\gamma_1[\rho_a^{(1)}(t_i; \mathbf{\alpha}^0)]$, in the distribution of $\rho_a^{(1)}(t_i; \mathbf{\alpha}^0)$ (left); and, (right) that of $\gamma_1[\rho_a^{(7)}(t_i; \mathbf{\alpha}^0)]$ in the distribution of $\rho_a^{(7)}(t_i; \mathbf{\alpha}^0)$.

As the plot on the left-side of Figure 10 indicates, the largest negative skewness in the distribution of $\rho_a^{(1)}(t_i; \mathbf{\alpha}^0)$ occurs at ca. 4.5 hours into the transient, and this negative skewness can be attributed overwhelmingly to the

uncertainties stemming from the parameter $\rho_{a,B}^{(in)}$ (as seen by Fig. 8). The second-largest negative skewness in the distribution of $\rho_a^{(1)}(t_i; \mathbf{\alpha}^0)$ occurs at ca. 7-7.5 hours into the transient, and this negative skewness can be attributed overwhelmingly to the uncertainties stemming from the parameter $\rho_{a,C}^{(in)}$ (see Figure 9). The third-largest negative “dip” in the skewness in the distribution of $\rho_a^{(1)}(t_i; \mathbf{\alpha}^0)$ occurs earlier in the transient, at ca. 3 hours into the transient; this negative “dip” stems from the uncertainties in the (assumed) normally-distributed model parameter $\rho_{a,A}^{(in)}$ (see Figure 7). These same features are evident in the plot of the skewness in the distribution of $\rho_a^{(7)}(t_i; \mathbf{\alpha}^0)$, near the inlet of the dissolver as depicted on the right-side of Figure 10. The three negative “dips” of varying magnitudes are similar to, but are much smaller and occur earlier in time than the negative “dips” in the distribution of $\rho_a^{(1)}(t_i; \mathbf{\alpha}^0)$. The three “dips” in the skewness of the distribution of $\rho_a^{(7)}(t_i; \mathbf{\alpha}^0)$, are caused by the uncertainties in the same parameters (sequentially in time) $\rho_{a,A}^{(in)}$, $\rho_{a,B}^{(in)}$, and $\rho_{a,C}^{(in)}$. In conclusion, the combination of 2nd-order sensitivities and uncertainties in $\rho_{a,A}^{(in)}$, $\rho_{a,B}^{(in)}$, and $\rho_{a,C}^{(in)}$ are the most important, in this order, in contributing to the marked negative dips in the skewness of the acid concentration response distributions. The effects of the combination of 2nd-order sensitivities and uncertainties in $\rho_{a,B}^{(in)}$, $\rho_{a,C}^{(in)}$, and $\rho_{a,A}^{(in)}$ increase in strength for the acid concentrations in the compartments furthest away from the inlet.

V. CONCLUSIONS AND OUTLOOK

The results of Section 4 present data for why it’s important to characterize the risk with using base case calculations to support decisions regarding dissolver/model performance. Non-zero skewness implies an asymmetric distribution of responses; in the case of the nitric acid concentration responses the respective asymmetries are negative, meaning that respective distributions favor values smaller than mean values. In other words assuming a Gaussian distribution for the response distributions would be misleading impacting activities such as; coupling the dissolver to other physico-mechanical models, adding equations for accounting for fission materials and gasses, or using measurements to “inversely” verify declarations with these calculations.

This work establishes and documents the dissolver model’s performance and accuracy for simulating nitric acid concentrations needed to dissolve spent nuclear fuel which in turn suggest accuracy in generating the source terms for key reprocessing facility components downstream. Clearly,

if non-Gaussian features of responses are to be captured and characterized then the computation of the 2nd-order responses sensitivities to the model parameters are essential. A new method which extends the 1st-order ASAM using adjoint operators, for computing most efficiently the exact 2nd-order sensitivities of the acid concentration in the surrogate dissolver model enables the computation of all of the 2nd-order response sensitivities exactly and efficiently, requiring at most $(N_\alpha + 1)$ adjoint computations, as

opposed to $(N_\alpha + 1)(N_\alpha + 2)/2$ forward computations required if using finite-difference formulas. The 2nd-order sensitivities impact the moments of the response distribution causing the “expected value of the response” to differ from the “computed nominal value of the response, albeit generally less than 1st order sensitivities, but are shown here to be the leading contributions to the third-order moment, or skewness of response distributions from uncorrelated and normally distributed parameters.

In the case of the full dissolver model developed and analyzed in this work, Gaussian-based confidence intervals would be very misleading for the times into the transient behavior of the acid concentration in the dissolver, particularly around the middle of the transient (around 3.5 to 4.5 hours after the initiation of the transient) and towards the last third of the transient (after 6 to 7.5 hours) that lasts for 10.5 hours, since the response skewness becomes large and negative over these times. Different procedures, based on chi-squared (with few degrees of freedom) or other asymmetric distributions would be needed to establish confidence intervals at these particularly important times.

Thinking about nuclear fuel reprocessing on a facility level scale, the aforementioned source terms might include actinide concentrations, fission gases, material inventories, etc., which either would be used to understand operational performance for reprocessing or be used for activities such as better understanding material accountability for international nuclear safeguards. Quantifying the accuracy of measurements and computations, as well as understanding their value for minimizing ignorance or risk would be key to assigning accurate confidence intervals and using these data beyond a paper study regardless of their intended application. In particular, ongoing work is aimed at extending and coupling the dissolver model analyzed here to other key reprocessing facility components, including condenser, solvent extractor, and evaporator, which will, in turn, be coupled to a cooling tower and atmospheric transport models for a full component capability to model aqueous nuclear fuel reprocessing. Future work will extend the application of the forward and inverse predictive modeling methodology of Cacuci and Ionescu-Bujor⁵ and its applications to multiple components of nuclear facilities for use in more comprehensive nuclear safeguard applications.

ACKNOWLEDGEMENTS

The authors very much wish to thank A.F. and M.C. Badea for verifying the computations presented in this work.

REFERENCES

1. J. J. PELTZ, and D. G. CACUCI “Predictive Modeling Applied to a Paradigm Spent Fuel Dissolver Model: I. Adjoint Sensitivity Analysis,” *Nucl. Sci. Eng.*, 183(2), 305-331, 2016. doi:10.13182/NSE15-98.
2. J. J. PELTZ, D. G. CACUCI, A. F. BADEA, and M. C. BADEA, “Predictive Modeling Applied to a Paradigm Spent Fuel Dissolver Model: II. Uncertainty Quantification and Reduction,” *Nucl. Sci. Eng.*, 183(3), 332-346, 2016. doi: 10.13182/NSE15-99.
3. J. J. PELTZ, and D. G. CACUCI, “Inverse Predictive Modeling of a Spent Fuel Dissolver Model,” *Nucl. Sci. Eng.*, 184(1), 1-15, 2016.
4. J. J. PELTZ, M. C. BADEA, D. G. CACUCI, and A. F. BADEA. “Predictive Modeling of a Paradigm Spent Fuel Dissolver” 2016 International Congress on Advances in Nuclear Power Plants (ICAPP 2016) 2016.
5. D. G. CACUCI and M. IONESCU-BUJOR, “Model Calibration and Best-Estimate Prediction Through Experimental Data Assimilation: I. Mathematical Framework,” *Nucl. Sci. Eng.*, 165, 18-44, 2010.
6. D. G. CACUCI, “Sensitivity theory for nonlinear systems: I. Nonlinear functional analysis approach,” *J., Math. Phys.*, 22, 2794–2802, 1981.
7. D. G. CACUCI, “Sensitivity theory for nonlinear systems: II. Extensions to additional classes of responses,” *J. Math. Phys.* 22, 2803–2812, 1981; see also D. G. CACUCI, *Sensitivity and Uncertainty Analysis: Theory*, Vol. 1, Chapman & Hall/CRC, Boca Raton, 2003.
8. D. G., CACUCI “Predictive Modeling of Coupled Multi-Physics Systems: I. Theory”, *Annals of Nucl. Energy*, 70, 266–278, 2014.
9. D. G., CACUCI, A. F. BADEA, M. C. BADEA, and J. J. PELTZ, “Efficient Computation of Operator-Type Response Sensitivities for Uncertainty Quantification and Predictive Modeling: Illustrative Application to a Spent Nuclear Fuel Dissolver Model,” *International Journal for Numerical Methods in Fluids*, (2017). doi: 10.1002/flid.4258.
10. D. G. CACUCI, “Sensitivity theory for nonlinear systems: II. Extensions to additional classes of responses”. *J., Math. Phys.* 22, 2803–2812, 1981.